FINSIM—a FORTRAN Program for Simulating Stochastic Acceleration Time Histories from Finite Faults

Igor A. Beresnev and Gail M. Atkinson
Carleton University, Ottawa, Canada

INTRODUCTION

Ground motions from earthquakes are created by ruptures on tectonic faults. The causative faults can be considered point sources at distances large compared to the fault dimensions. At closer distances, the finite-fault effects become important. These effects are primarily related to the finite speed of rupture propagation, which causes certain parts of the fault to radiate energy much earlier than do other parts; the delayed waves then interfere, creating significant directivity effects. The duration and amplitude of ground motion become dependent on the angle of observation.

Finite-source modeling has been an important part of ground-motion prediction near the epicenters of large earthquakes (Hartzell, 1978; Irikura, 1983; Joyner and Boore, 1986; Heaton and Hartzell, 1989; Somerville *et al.*, 1991; Hutchings, 1994; Tumarkin and Archuleta, 1994; Zeng *et al.*, 1994). In the approach adopted in most studies, the fault plane is discretized into elements, each element is treated as a small source, and the radiation from all subsources is summed, with proper time delays. The rupture starts at a given point on the fault (hypocenter) and propagates with constant velocity, triggering subsources as soon as it reaches them. This simple "kinematic" idea stimulated numerous implementations that differ chiefly in how the subsource spectra or how path effects are defined (Beresnev and Atkinson, 1997 give a more detailed review).

One of the possible alternative approaches is to characterize subevents as "stochastic" ω^2 sources and to use the empirical distance-dependent duration, geometric spreading, and attenuation (Q) models to describe path effects. The stochastic simulation method has been successfully applied to ground-motion prediction from earthquakes that could be treated as point sources (Hanks and McGuire, 1981; Boore, 1983; Boore and Atkinson, 1987; Boore, 1996). The purpose of *FINSIM* is to extend this technique to large faults by using the procedure outlined in Beresnev and Atkinson (1997). A similar approach has been implemented by Silva *et al.* (1990) and Schneider *et al.* (1993), with the differences being in how the moments and corner frequencies of ω^2 sources are introduced and linked to subfault size.

METHOD

The simulation method used in the program is described in detail in Beresnev and Atkinson (1997) and in previous publications on the foundations of the stochastic technique. Subsource time series are generated through the procedure of Boore (1983, 1996), assuming an underlying ω^2 spectrum, and propagated to the observation point using specified duration and attenuation operators (Boore and Atkinson, 1987). The program employs a standard summation procedure, in which the rupture propagates radially from the hypocenter, triggering subsources as it passes them. A random component is included in the subsource trigger times (Beresnev and Atkinson, 1997). The program either generates ground motion for a "hard-rock" site condition or the user may specify frequency-dependent site amplification factors.

A key component of the model concerns the procedure by which the equivalent ω^2 sources are assigned to fault elements. The program starts with the fault discretization model, in which the fault plane is subdivided into elements having length Δl and width Δw, specified by the user. We will assume here for simplicity that $\Delta l = \Delta w$. Each element, having a finite area Δl^2, is assigned an ω^2 spectrum with a certain moment and corner frequency.

The program determines the subfault moment (m_0) from its definition

$$m_0 = \Delta\sigma \, \Delta l^3 \qquad (1)$$

where $\Delta\sigma$ is the "stress" parameter, or a coefficient relating subfault moment to its size. It has the dimension of stress, but we caution against attributing $\Delta\sigma$ any other physical meaning except for that defined in Equation (1) (Atkinson and Beresnev, 1997; Beresnev and Atkinson, 1997). The stress parameter is most closely related to the static stress drop, as employed by Kanamori and Anderson (1975). The program sets $\Delta\sigma$ to a constant of 50 bars, close to the "average" suggested by Kanamori and Anderson (1975, Figure 2).

The program determines the corner frequency of the subfault spectrum (f_0) from

$$f_0 = \frac{\left(\frac{yz}{\pi}\right)\beta}{\Delta l} \tag{2}$$

where β is the shear-wave velocity and y is the fraction of rupture-propagation velocity to β, normally set to a value of 0.8 (Beresnev and Atkinson, 1997).

In our initial formulation, the parameter z in Equation (2) was a constant needing calibration. In subsequent refinements, we have linked z to the maximum rate of slip on the fault, which attributes to this parameter a direct physical meaning. The rate (time derivative) of dislocation that radiates an ω^2 spectrum is given by Equation (8) of Beresnev and Atkinson (1997), where $n = 1$. The maximum rate (v_m) is $v_m = U/e\tau$, where U is the final dislocation displacement, e is the base of the natural logarithm, and $\tau \equiv 1/2\pi f_0$. Using Equation (2) and the definition of the stress parameter $\Delta\sigma \equiv \mu(U/\Delta l)$, where μ is the shear modulus, we find

$$v_m = \left(\frac{2yz}{e}\right)\left(\frac{\Delta\sigma}{\rho\beta}\right), \tag{3}$$

where ρ is the density. Equation (3) relates the maximum slip rate on the fault to the parameter z. As follows from shear-dislocation theory, z has a value of 1.68 for an ω^2 model, using standard conventions for the definition of the dislocation rise time (Beresnev and Atkinson, 1997). The value of z is important, because it controls the level of high-frequency radiation. The program allows z to vary, which physically means that the maximum slip rate on the modeled fault may be varied. If a "standard" rupture is to be modeled, z should be left at its standard value of 1.68. The quantity z may have significant uncertainty: v_m is poorly constrained even for past well-recorded earthquakes.

A significant issue for virtually all finite-fault simulation methods concerns the choice of the subfault size used in the simulation. The effect of Δl on radiated spectral amplitudes can be estimated as follows. The Fourier acceleration spectrum at a distance R from a subsource has an ω^2 shape: $a(f) = Cm_0 f^2/[1+(f/f_0)^2]$ (Boore, 1983), where C is a constant given by $C = 4\pi^2 R^{\theta\phi}/4\pi\rho\beta^3 R$, and $R^{\theta\phi}$ is the radiation pattern. Substituting m_0 and f_0 from Equations (1)–(2) gives

$$a(f) = \frac{C\Delta\sigma f^2 \Delta l^3}{1+\left(\frac{\pi}{yz\beta}\right)^2 f^2 \Delta l^2}. \tag{4}$$

Finally, the radiation from N subsources should be summed to reach the specified target moment (M_0). *FINSIM* determines N from

$$N = \frac{M_0}{m_0} = \frac{M_0}{\Delta\sigma\Delta l^3}. \tag{5}$$

At high frequencies (above the corner frequencies of the subfaults), the spectra add incoherently, leading to a total amplitude increase of $N^{1/2}$ (Joyner and Boore, 1986). Multiplying (4) by $N^{1/2}$ from (5) and neglecting the unity in the denominator, we have a finite-fault spectrum of the form

$$a(f) = C\left(\Delta\sigma M_0\right)^{1/2}\left(\frac{yz\beta}{\pi}\right)^2 \Delta l^{-1/2}. \tag{6}$$

Equation (6) shows that the amplitude of summed radiation has a square-root dependence on Δl. This corrects our previous conclusion that it is subfault-size independent (Beresnev and Atkinson, 1997).

To ensure uniqueness of simulations, a range of Δl used should be constrained. There is general agreement that the subsource size in the stochastic method should correspond to M 5–6.5 earthquakes, depending upon the size of target event (Silva *et al.*, 1990; Schneider *et al.*, 1993). This constitutes a rather empirical rule, based on numerous validation studies. It can be given a theoretical justification as follows.

The lower bound on Δl comes from the requirement that the corner frequency of the subsources lie below the frequency range of interest, a condition leading to Equation (6). If f_0 moves into the simulated frequency range, the sensitivity of the method to subfault size significantly increases. *FINSIM* carries out simulations for frequencies above 0.25 Hz. At this value, Equation (2) gives a minimum subfault size of Δl = 6.3 km, assuming the "standard" values of y and z and β = 3.7 km/sec. Since this is only a rough estimate, *FINSIM* sets the lower limit at 5 km. From the empirical relationship between fault area and moment magnitude (Wells and Coppersmith, 1994), this minimum size corresponds to an event of approximately magnitude M 5.4.

An upper bound on Δl also exists. The simulation requires a reasonable number of subevents to be summed in order to obtain a realistic shape for the accelerogram. From Equation (5), the number of subsources (N) is proportional to Δl^{-3}. A large value for Δl leads to a very small number of subfaults needed to achieve the target moment. Our tests showed that, for a large variety of target moments, finite-fault dimensions, and slip distributions, the resulting accelerogram is adequately populated with subevent time histories if Δl is less than approximately 15 km. This corresponds to a moment magnitude of M 6.4 (Wells and Coppersmith, 1994).

In general, then, *FINSIM* should be used with Δl lying in the range from 5 to 15 km, approximately. This leaves a simulation uncertainty which is bounded by about a factor of $\sqrt{3}$ from the low to the high ground-motion amplitudes, related entirely to the ambiguity in specifying the subfault size. We consider this an acceptable level of uncertainty.

It also follows that the program models seismic events with magnitudes exceeding approximately M 5.4. Smaller earthquakes can be effectively considered "point sources." Interestingly, this is the magnitude level ($\sim M$ 5.5), beyond which a point-source model starts to significantly deviate from empirical source spectra, as shown for California earthquakes by Atkinson and Silva (1997).

The model constraints have been calibrated against ground motion from well-recorded large earthquakes. Our validation studies showed that the stochastic finite-fault technique, for the default parameters given above, accurately reproduces ground motions from a number of significant events, including the M 8.1 1985 Michoacan (Mexico), M 8.0 1985 Valparaiso (Chile), M 5.8 1988 Saguenay (Québec) events (Beresnev and Atkinson, 1997), and M 6.7 1994 Northridge, California earthquake (Beresnev and Atkinson, 1998). An example of a validation test is given below.

INPUT AND OUTPUT PARAMETERS

The *FINSIM* input parameters are prepared in a file. The target fault is assumed to have a rectangular shape with horizontal upper and lower sides. The program requires:

- geometry of target fault (strike, dip, length, width, depth of upper edge);
- target magnitude;
- fault location (geographic coordinates of one of its corners);
- geographic coordinates of the observation point;
- number of subfaults along strike and dip;
- position of the hypocenter;
- slip distribution (if not specified, program generates random slip);
- average crustal density and shear-wave velocity;
- radiation-strength factor controlling the value of parameter z (maximum rate of slip);
- crustal Q model in the form $Q(f) = Q_0 f^{\eta}$;
- geometric attenuation model $1/R^{\alpha}$, where α is allowed to vary depending on range of distances from fault;
- subsource-radiation duration model, incorporating a linear increase of duration with distance, with slopes depending on distance range;
- parameter of "fmax" or "kappa" filter;
- option for tapered boxcar or Saragoni-Hart window for subsource time histories;
- sampling interval;
- interval of frequencies and percentage of critical damping for response spectrum calculation;
- number of simulation trials for calculating average response spectrum;
- name of ASCII file containing frequency-dependent amplification function by which generated motions are amplified. Two separate amplifications are allowed, accounting, for example, for generic crustal amplification and local site response.

The output of the program is given in separate ASCII files containing the horizontal-component acceleration time history, the average response spectrum, and the summary of input parameters.

VALIDATION EXAMPLE: 1985 MEXICO EARTHQUAKE

As an example of *FINSIM*'s performance, we show results of the simulation of ground motions at the Caleta de Campos station for the M 8.1 1985 Michoacan, Mexico earthquake (Anderson *et al.*, 1986). At a distance of approximately 14 km, this was the closest station to the fault rupture, which had an area of approximately 150 × 140 km (Somerville *et al.*, 1991). More validation examples are provided by Beresnev and Atkinson (1997). Our intention is to present this simulation as a "blind" comparison. We have made no attempt to tailor any "generic" values of parameters, discussed above, for this particular application. The only parameter that has been controlled is the cut-off frequency f_m of the "fmax" filter (see Boore, 1983, for its definition). f_m in the simulation is set to 10 Hz, instead of 15 Hz characteristic of western North America (Boore, 1983). This specific value affects simulation results only at frequencies near or above 10 Hz. The generic parameters are those given as program defaults, as described in the previous sections.

The geometry of the target fault and slip distribution during the Michoacan earthquake are taken from Somerville *et al.* (1991) and summarized by Beresnev and Atkinson (1997). The subfault length and width are 15 and 14 km, respectively, leading to 100 subfaults on the fault plane. The actual number of subfaults summed, accounting for inhomogeneous slip distribution, is 86. One trial has been used to compute the response spectrum of the simulated record.

Figure 1 shows the simulated and observed pseudo-acceleration response spectra and accelerograms. The shape and amplitude of the observed spectrum are simulated closely. The duration and shape of the acceleration record are also reproduced quite well.

Figure 2 is the result of the same simulation with the subfault length and width reduced by a factor of two (to 7.5 and 7 km, respectively). The total number of subfaults on the fault plane is 400; there are 732 subevents summed. The amplitude level of the radiation is increased compared to Figure 1, in accordance with Equation 6, illustrating the dependence of the simulation results on the subfault size. However, this uncertainty level may be considered small compared to that introduced by the possible variability in the maximum slip rate for future earthquakes. To illustrate this, we note that the level of radiation is controlled by the quantity z^2, or v_m^2 (Equations 3 and 6). It follows that a change in maximum slip velocity of, say, a factor of two will lead to a factor of four change in the amplitude of the radiated spectrum. Coupled with the unknown geometry of future rupture zones, this becomes a chief source of uncertainty in ground-motion forecasts.

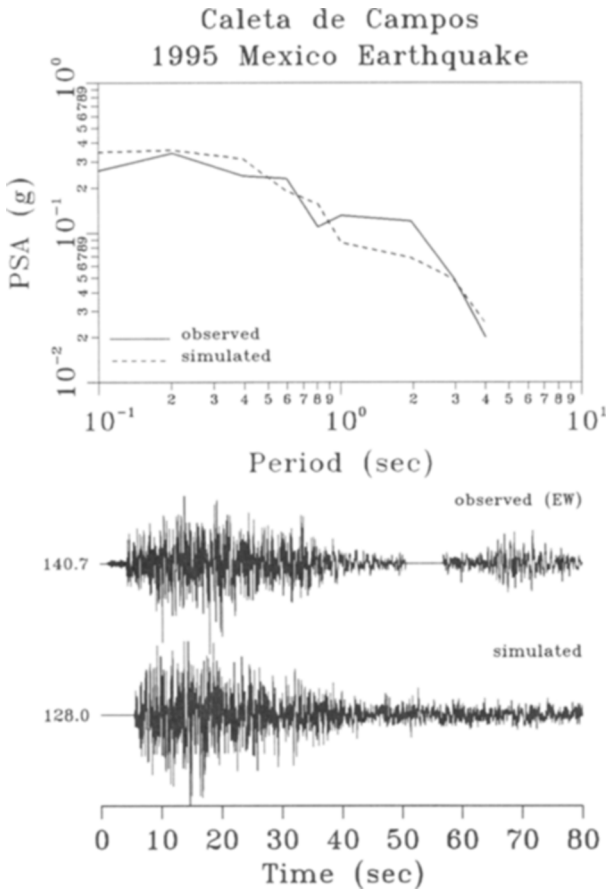

▲ **Figure 1**. Simulated and observed 5%-damped pseudo-acceleration response spectra and horizontal acceleration time histories for the Caleta de Campos station during the *M* 8.1 1985 Michoacan (Mexico) earthquake. The numbers to the left of the traces indicate peak horizontal acceleration in cm/sec^2.

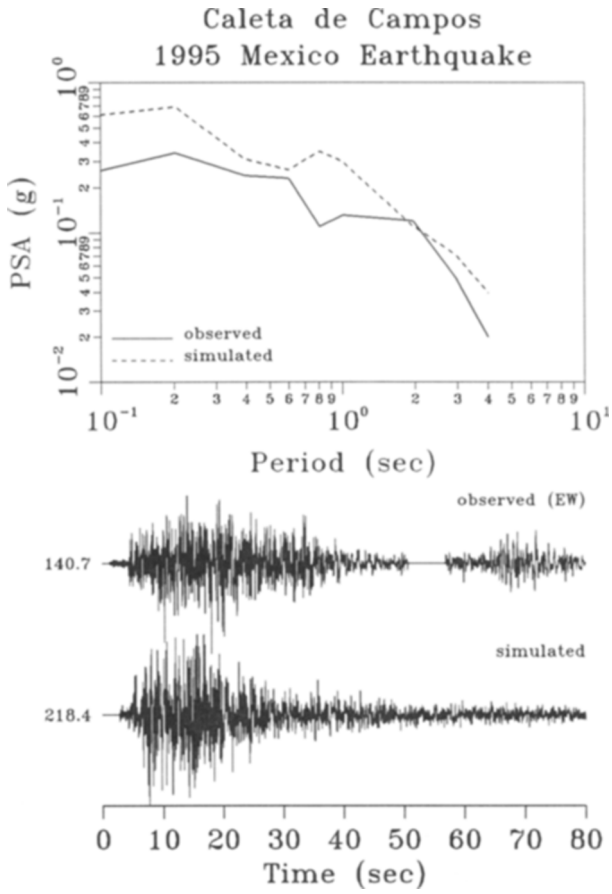

▲ **Figure 2**. Same as Figure 1, except subfault dimensions are reduced by a factor of two.

Finally, we check whether the value of z used above is consistent with the actual velocity observed on the Michoacan fault. The generic conditions used imply $\gamma = 0.8$, $z = 1.68$, $\Delta\sigma = 50$ bars, $\rho = 2.8$ g/cm^3, $\beta = 3.7$ km/sec. Equation (3) then gives $v_m \approx 0.5$ m/sec. The actual maximum slip rate that occurred during the Michoacan earthquake can be assessed by dividing the estimated maximum displacement by the rise time. Heaton (1990) and Somerville *et al.* (1991) assess the rise time as 5 and 10 sec, respectively. The estimate of maximum displacement is 6.5 m (Somerville *et al.*, 1991). This provides the maximum slip velocity in the range of 0.65 to 1.3 m/sec, which agrees satisfactorily with the value of 0.5 m/sec obtained above.

GROUND-MOTION FORECAST: LARGE EARTHQUAKE ON THE CASCADIA SUBDUCTION ZONE

We also provide an example of the use of *FINSIM* for a truly "blind" prediction, or simulation of ground motion from a future event. For this purpose, we examine the case of a large earthquake on the Cascadia subduction zone (*i.e.*, the United States Pacific Northwest region and Canada's southwest British Columbia). This is a case of significant practical interest (Hyndman, 1995).

Using recent geophysical data, Hyndman and Wang (1995) delineated the spatial extent of the Cascadia seismogenic zone. Following their results, we use a target fault that has a strike of 310° and dip of 10°, covers the depth range of 5 to 33 km, and covers an area 300 by 160 km along strike and dip, respectively. The modeled fault rupture breaks the maximum width of the seismogenic zone, including both the locked and the transition areas (Hyndman and Wang, 1995). The target magnitude is 8.2. The subfault length and width are 12 and 16 km, respectively, implying 250 subfaults on the fault plane. All the "standard" parameters, as for the Michoacan earthquake, are assumed; f_m is set to its average western North America value of 15 Hz (Boore, 1983). The illustrative simulation is done for Vancouver, British Columbia, located at distances of 150 to 400 km from the fault plane.

Figure 3 shows the simulated 5%-damped response spectra for ten random slip distributions and hypocenter locations (solid lines). The acceleration time history shown corresponds to one of these scenarios. All simulation results have been

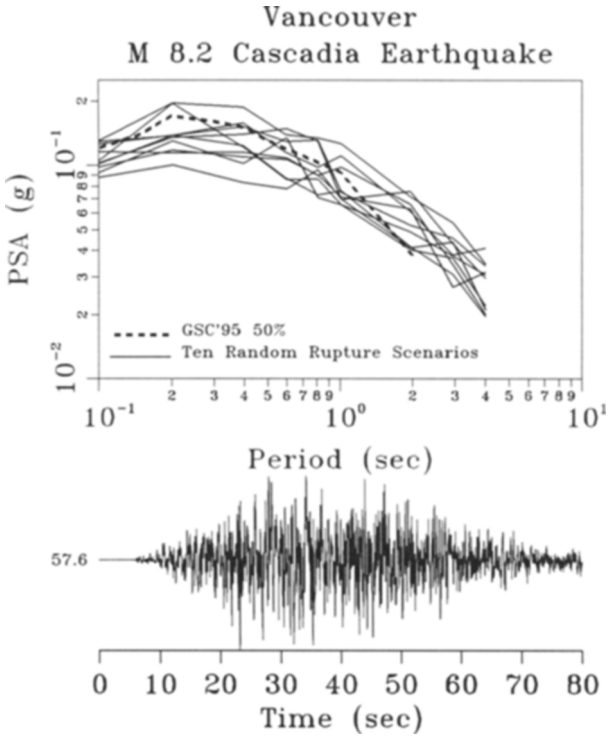

▲ **Figure 3**. Simulated 5%-damped pseudo-acceleration response spectra and acceleration time history at Vancouver, British Columbia from the hypothetical *M* 8.2 Cascadia subduction zone earthquake. *FINSIM* simulations corresponding to ten randomly-generated slip distributions are shown by solid lines. The time history is for one scenario. The dashed line shows 50-percentile response spectral values for the similar earthquake predicted by Adams *et al.* (1996). All data shown are for Class B ("firm ground") soil site.

multiplied by the generic western North America crustal amplification function (Boore and Joyner, 1997). For the sake of comparison, Figure 3 also presents 50-percentile response spectra for the hypothetical Cascadia subduction zone earthquake with the same magnitude, estimated by Adams *et al.* (1996) from the empirical ground-motion relationships of Crouse (1991) (dashed line). Since the Adams *et al.*'s (1996) curve is presented for a generic "firm soil" condition (Class B of Boore *et al.*, 1993), we have additionally amplified the simulated records using the Class B amplification functions. As seen from Figure 3, the variability in rupture scenarios, estimated from *FINSIM*, leads to approximately a factor of two variability in spectral amplitudes of ground motion at Vancouver. The *FINSIM* simulations and the reference curve from Adams *et al.* (1996) agree well.

SUMMARY

FINSIM simulates ground motion near ruptures of large earthquakes having finite dimensions. The simulated range of frequencies lies above approximately 0.25 Hz. The program produces horizontal acceleration time histories and response spectra at a rock or soil site for the desired earthquake scenario.

The program generalizes the stochastic ground-motion simulation technique, developed for point sources, to the case of finite faults. It subdivides the large fault plane into subfaults and assumes each subfault to be a point source with an ω^2 spectrum. A random component is added to the subfault spectra to simulate complexity in the ground-motion generation process. The subsources are summed over the fault plane to produce a simulated record for an event of the specified target moment.

Flexibility in the specification of the input parameters makes it easy to tailor the program to region-specific applications. For example, the distance-dependent subsource duration, geometric spreading, and attenuation (Q) models may be established from empirical studies of small-magnitude seismicity for a variety of regions; this information is entered as input to the program. The program also allows the user to specify the slip distribution on the fault-plane, or to internally generate a random slip. The level of high-frequency radiation is controlled by a parameter that is determined by the maximum slip velocity on the fault. In the prediction of "median" ground-motion for future events, this parameter can be left at its "standard" value.

FINSIM is available to any interested parties by writing to the authors. We provide the FORTRAN source code and an example of the input file with the detailed parameter description. We also provide examples of output information, including simulated accelerogram and pseudo-acceleration response spectrum for one particular simulation case. ■

ACKNOWLEDGMENTS

This work was supported by the Natural Sciences and Engineering Research Council of Canada. The authors are grateful to David Boore, who shared with us certain subroutines from his code SMSIM. The observed acceleration time histories at the Caleta de Campos station during the Mexico earthquake were obtained from the Guerrero Accelerograph Network database at the Seismological Laboratory, University of Nevada at Reno (http://www.seismo.unr.edu/). J. Ebel provided a thorough review of the paper.

REFERENCES

Adams, J., D.H. Weichert, S. Halchuk, and P.W. Basham (1996). Trial seismic hazard maps of Canada - 1995: Final values for selected Canadian cities, *Geological Survey of Canada Open File Report 3283*, 97 pp.

Anderson, J.G., P. Bodin, J.N. Brune, J. Prince, S.K. Singh, R. Quaas, and M. Onate (1986). Strong ground motion from the Michoacan, Mexico, earthquake, *Science*, **233**, 1043–1049.

Atkinson, G.M. and I.A. Beresnev (1997). Don't call it stress drop, *Seism. Res. Lett.*, **68**, 3–4.

Atkinson, G.M. and W. Silva (1997). An empirical study of earthquake source spectra for California earthquakes, *Bull. Seism. Soc. Am.*, **87**, 97–113.

Beresnev, I.A. and G.M. Atkinson (1997). Modeling finite fault radiation from the ω^n spectrum, *Bull. Seism. Soc. Am.*, **87**, 67–84.

Beresnev, I.A. and G.M. Atkinson (1998). Stochastic finite-fault modeling of ground motions from the 1994 Northridge, California earthquake. I. Validation on rock sites, *Bull. Seism. Soc. Am.* (submitted).

Boore, D.M. (1983). Stochastic simulation of high-frequency ground motions based on seismological models of the radiated spectra, *Bull. Seism. Soc. Am.*, **73**, 1865–1894.

Boore, D.M. (1996). SMSIM - Fortran programs for simulating ground motions from earthquakes: version 1.0, *US Geological Survey Open File Report 96-80-A*, 73 pp.

Boore, D.M. and G.M. Atkinson (1987). Stochastic prediction of ground motion and spectral response parameters at hard-rock sites in eastern North America, *Bull. Seism. Soc. Am.*, **77**, 440–467.

Boore, D., W. Joyner, and T. Fumal (1993). Estimation of response spectra and peak accelerations from western North American earthquakes: an interim report, *US Geological Survey Open File Report 93-509*.

Boore, D.M and W.B. Joyner (1997). Site amplifications for generic rock sites, *Bull. Seism. Soc. Am.*, **87**, 327–341.

Crouse, C.B. (1991). Ground-motion attenuation equations for Cascadia subduction zone earthquakes, *Earthquake Spectra*, **7**, 201–236.

Hanks, T.C. and R.K. McGuire (1981). The character of high frequency strong ground motion, *Bull. Seism. Soc. Am.*, **71**, 2071–2095.

Hartzell, S.H. (1978). Earthquake aftershocks as Green's functions, *Geophys. Res. Lett.*, **5**, 1–4.

Heaton, T.H. (1990). Evidence for and implications of self-healing pulses of slip in earthquake rupture, *Phys. Earth Planet. Interiors*, **64**, 1–20.

Heaton, T.H. and S.H. Hartzell (1989). Estimation of strong ground motions from hypothetical earthquakes on the Cascadia subduction zone, Pacific Northwest, *Pure Appl. Geophys. (Pageoph)*, **129**, 131–201.

Hutchings, L. (1994). Kinematic earthquake models and synthesized ground motion using empirical Green's functions, *Bull. Seism. Soc. Am.*, **84**, 1028–1050.

Hyndman, R.D. (1995). Giant earthquakes of the Pacific Northwest, *Scientific American*, **273**, No.6, 50–57.

Hyndman, R.D. and K. Wang (1995). The rupture zone of Cascadia great earthquakes from current deformation and the thermal regime, *J. Geophys. Res.*, **100**, 22,133–22,154.

Irikura, K. (1983). Semi-empirical estimation of strong ground motions during large earthquakes, *Bull. Disaster Prevention Res. Inst. (Kyoto Univ.)*, **33**, 63–104.

Joyner, W.B. and D.M. Boore (1986). On simulating large earthquakes by Green's-function addition of smaller earthquakes, in *Proc. Fifth Maurice Ewing Symposium on Earthquake Source Mechanics*, S. Das, J. Boatwright, and C. Scholz, Editors, Am. Geophys. Union, 269–274.

Kanamori, H. and D.L. Anderson (1975). Theoretical basis of some empirical relations in seismology, *Bull. Seism. Soc. Am.*, **65**, 1073–1095.

Schneider, J.F., W.J. Silva, and C. Stark (1993). Ground motion model for the 1989 *M* 6.9 Loma Prieta earthquake including effects of source, path, and site, *Earthquake Spectra*, **9**, 251–287.

Silva, W.J., R. Darragh, and I.G. Wong (1990). Engineering characterization of earthquake strong ground motions with applications to the Pacific Northwest, in *Proc. Third NEHRP Workshop on Earthquake Hazards in the Puget Sound/Portland Region*, W. Hays, Editor, *US Geological Survey Open File Report.*

Somerville, P., M. Sen, and B. Cohee (1991). Simulations of strong ground motions recorded during the 1985 Michoacán, Mexico and Valparaíso, Chile, earthquakes, *Bull. Seism. Soc. Am.*, **81**, 1–27.

Tumarkin, A.G. and R.J. Archuleta (1994). Empirical ground motion prediction, *Annali di Geofisica*, **37**, 1691–1720.

Wells, D.L. and K.J. Coppersmith (1994). New empirical relationships among magnitude, rupture length, rupture width, rupture area, and surface displacement, *Bull. Seism. Soc. Am.*, **84**, 974–1002.

Zeng, Y., J.G. Anderson, and G. Yu (1994). A composite source model for computing realistic strong ground motions, *Geophys. Res. Lett.*, **21**, 725–728.

Department of Earth Sciences
Carleton University
1125 Colonel By Drive
Ottawa, Ontario
K1S 5B6, Canada
(beresnev@ccs.carleton.ca; gma@ccs.carleton.ca)